AIP Journal of Applied Physics

Microstructure and electrical properties of Aurivillius phase (CaBi 2 Nb 2 O 9) 1 − x (BaBi 2 Nb 2 O 9) x solid solution

Hongtao Zhang, Haixue Yan, and Michael J. Reece

Citation: Journal of Applied Physics **108**, 014109 (2010); doi: 10.1063/1.3457229
View online: http://dx.doi.org/10.1063/1.3457229
View Table of Contents: http://scitation.aip.org/content/aip/journal/jap/108/1?ver=pdfcov
Published by the AIP Publishing

Microstructure and electrical properties of Aurivillius phase $(CaBi_2Nb_2O_9)_{1-x}(BaBi_2Nb_2O_9)_x$ solid solution

Hongtao Zhang,[1,2] Haixue Yan,[1,3] and Michael J. Reece[1,3,a)]
[1]*School of Engineering and Materials Science, Queen Mary University of London, London E1 4NS, United Kingdom*
[2]*Department of Materials, University of Oxford, Oxford, OX1 3PH, United Kingdom*
[3]*Nanoforce Technology Ltd., London E1 4NS, United Kingdom*

(Received 25 February 2010; accepted 29 May 2010; published online 12 July 2010)

The microstructures and electrical properties of Aurivillius phase ferroelectric solid solutions of $(CaBi_2Nb_2O_9)_{1-x}(BaBi_2Nb_2O_9)_x$ $(0 \le x \le 1)$ have been studied. X-ray diffraction analyses revealed a bismuth layered structure for all compositions. Scanning electron microscope images showed randomly oriented and platelike grain morphology. The Curie point T_c or the maximum permittivity temperature T_m decreased with increasing x. The $(CaBi_2Nb_2O_9)_{1-x}(BaBi_2Nb_2O_9)_x$ ceramics exhibited a ferroelectric–paraelectric phase transition at small x values $(x \le 0.5)$, whereas a relaxor behavior was observed at high x values $(x \ge 0.8)$. The d_{33} value of $CaBi_2Nb_2O_9$ ceramics was enhanced by Ba^{2+} doping on the A-sites $(x \le 0.3)$. A combination of high d_{33} values and high T_c points (>700 °C) suggests that compositions with $x \le 0.3$ could be good candidates for high-temperature piezoelectric applications. The composition with $x=0.8$ is a relaxor ferroelectric with T_m around 320 °C at 1 MHz. © *2010 American Institute of Physics*. [doi:10.1063/1.3457229]

I. INTRODUCTION

Bismuth layer-structured ferroelectrics (BLSFs), with the general formula $(Bi_2O_2)^{2+}(A_{m-1}B_mO_{3m+1})^{2-}$, are an important family of lead-free ferroelectrics first identified by Aurivillius.[1] The structure of these compounds can be described as pseudo-perovskite $(A_{m-1}B_mO_{3m+1})^{2-}$ slabs separated by $(Bi_2O_2)^{2+}$ layers along the crystallographic c-axis. The 12-coordinated A site can be occupied by monovalent, divalent, or trivalent metallic cations. While the octahedral-coordinated B site can be occupied by tetravalent, pentavalent, or hexavalent metallic cations. The number of octahedra along the c-axis between two neighboring $(Bi_2O_2)^{2+}$ layers is indicated by m.[2] Aurivillius phase materials have generated increasing attention due to their potential use in nonvolatile ferroelectric random-access memory[3,4] and high-temperature piezoelectric applications[5] because of their fatigue-free properties and high Curie point, respectively. Some Aurivillius phase compounds show interesting relaxor and multiferroic properties when Ba/lanthanides[6,7] and Fe (Ref. 8) are on the A- and B-site in the general formula, respectively.

The origin of ferroelectricity in BLSFs is the displacement of the A site cations of the perovskite block with cooperative tilting of the BO_6 octahedra.[9,10] Compared with traditional piezoelectric ceramics, such as lead zirconate titanate and $BaTiO_3$, BLSFs compounds are characterized by low piezoelectric activity and electromechanical coupling factors and high coercive field because the rotation of the spontaneous polarization is restricted to the a-b plane.[11] It has been reported that BLSFs solid solution ceramics exhibit improved electrical properties compared to end-member compounds. For example, the mechanical quality factor Q_m reached a maximum value of 11000 at $x=0.75$ in solid solution of $(SrBi_2Ta_2O_9)_{1-x}(CaBi_2Ta_2O_9)_x$.[12] The Q_m and electromechanical coupling factors k_p were enhanced up to the maximum value of 13500 and 0.12, respectively, in $SrBi_2Ta_2O_9-Bi_3TiTaO_9$ solid solution system, $Sr_{x-1}Bi_{4-x}Ti_{2-x}Ta_xO_9$ $(1 \le x \le 2)$ at $x=1.25$.[13] The maximum k_p of 9.0% and Q_m of 7000 were obtained for $x=0.75$ in solid solution system $(Na_{0.5}Bi_{2.5}Ta_2O_9)_{1-x}(Sr_{0.8}Bi_{2.15}Ta_2O_9)_x$.[14] Solid solution of $(SrBi_2Ta_2O_9)_{1-x}(Bi_3TiNbO_9)_x$ exhibited at least one order lower conductivity in the temperature range of 400–900 °C than those of the end members $SrBi_2Ta_2O_9$ and Bi_3TiNbO_9 and remanent polarization (P_r) of $(SrBi_2Ta_2O_9)_{1-x}(Bi_3TiNbO_9)_x$ with $x=0.8$ was 14.4 $\mu C/cm^2$, which was higher than P_r (=11.8 $\mu C/cm^2$) of $SrBi_2Ta_2O_9$.[15] $(Bi_3TiNbO_9)_x(SrBi_2Nb_2O_9)_{1-x}$ solid solution ceramics with $x=0.6$ present a higher piezoelectric coefficient $(d_{33}=11$ pC/N) and lower coercive field $(E_c=67$ kV/cm) than those of Bi_3TiNbO_9 $(d_{33}=1-4$ pC/N, $E_c>75$ kV/cm).[16] In $(Bi_3TiNbO_9)_{1-x}(BaBi_2Nb_2O_9)_x$, much larger P_r value (6–7 $\mu C/cm^2$) was observed for $x=0.1-0.3$ compared with P_r (1 $\mu C/cm^2$) of Bi_3TiNbO_9. The resistivity for $x=0.2$ was one order larger than that of Bi_3TiNbO_9.[17]

In addition, compared to normal ferroelectrics, relaxor ferroelectrics (RFE) have attracted intensive interest due to their large dielectric permittivity and electromechanical constants for piezoelectric transducer and actuator applications.[18] But traditional RFE piezoelectrics, such as $Pb(Mg_{1/3}Nb_{2/3})O_3-PbTiO_3$ and $Pb(Zn_{1/3}Nb_{2/3})O_3-PbTiO_3$, are not suitable for application under harsh thermal conditions due to their relatively low T_m temperatures (<300 °C), at which there is the maximum of dielectric permittivity.[19,20] There are relatively few reports on relaxor behavior in BLSFs solid solution ceramics. The study of $(Na_{0.5}Bi_{4.5}Ti_4O_{15})_{1-x}(BaBi_4Ti_4O_{15})_x$ solid solutions $(m=4)$

a)Electronic mail: m.j.reece@qmul.ac.uk.

TABLE I. Optimal sintering temperatures and the highest densities of the $(CBNO)_{1-x}(BBNO)_x$ ceramics (The relative density is shown in parentheses).

x	Sintering temperature (°C)	Density (g/cm^3)
0	1150	6.82 (96.7%)
0.1	1150	6.87
0.3	1150	7.16
0.5	1100	6.90
0.8	1100	7.14
0.9	1100	7.27
1.0	1100	7.17 (96.9%)

indicated that the end member $Na_{0.5}Bi_{4.5}Ti_4O_{15}$ and $BaBi_4Ti_4O_{15}$ exhibited typical ferroelectric and RFE behaviors, respectively. While, relaxorlike behavior appears for $x \geq 0.6$.[21] But the ferroelectric and piezoelectric properties of $(Na_{0.5}Bi_{4.5}Ti_4O_{15})_{1-x}(BaBi_4Ti_4O_{15})_x$ solid solutions were not investigated.

As members of BLSFs with $m=2$, $CaBi_2Nb_2O_9$ (CBNO) and $BaBi_2Nb_2O_9$ (BBNO) are particularly interesting because they represent two extreme cases considering the average ionic radii of their A-site cations [$r^{2+}_{Ba}=1.61$ Å, $r^{2+}_{Ca}=1.34$ Å, coordination number=12] (Ref. 22) and their dielectric behaviors. CBNO and BBNO exhibit classic ferroelectric[23] and relaxor[24] behavior, respectively. Recently, we reported that CBNO has the highest-known Curie point (943 °C) among BLSFs and the highest thermal depoling temperature for polycrystalline ferroelectric ceramics.[23,25] This means that CBNO is a very promising material for high-temperature (up to 800 °C) piezoelectric applications. How to further improve the piezoelectric activity of CBNO ceramic without dramatically decreasing its high T_c is of great interest for commercial applications. We have also demonstrated that the polarization-electrical field ($P-E$) response of BBNO ceramics is dominated by lossy capacitor behavior and the piezoelectric constant d_{33} is zero after poling at room temperature.[24] The objective of the current research was to investigate for CBNO–BBNO solid solution if: (1) piezoelectric properties of CBNO can be improved while maintaining their high T_c and (2) RFE behavior occurs with $T_m > 300$ °C. In the present study, we present a systematic study of the microstructure and electrical properties of solid solutions in the CBNO–BBNO series with above two aims.

II. EXPERIMENTAL

Polycrystalline ceramic samples with the formula of $(CBNO)_{1-x}(BBNO)_x$ where $x=0$, 0.1, 0.3, 0.5, 0.8, 0.9, and 1.0 were prepared by conventional solid-state reaction sintering. The starting materials were $CaCO_3$ of 99.0% purity, $BaCO_3$ of 99.0% purity, Bi_2O_3 of 99.975% purity, and Nb_2O_5 of 99.9% purity. The powders were ball milled for 12

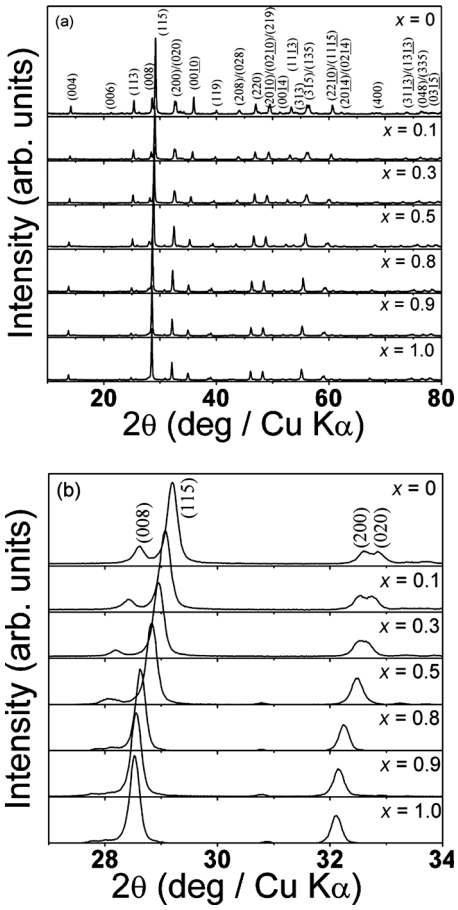

FIG. 1. XRD patterns of $(CBNO)_{1-x}(BBNO)_x$ ceramics as a function of x: (a) $2\theta=10°-80°$ and (b) $2\theta=27°-34°$.

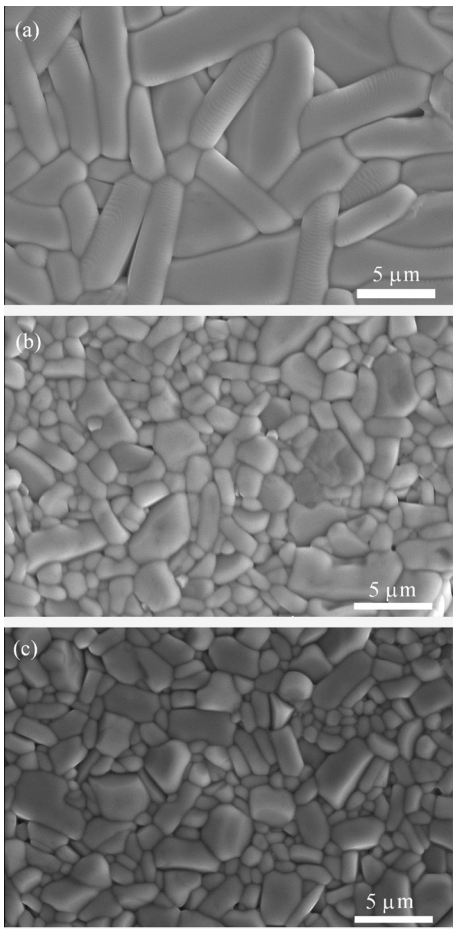

FIG. 2. Secondary electron SEM micrographs showing typical microstructures of $(CBNO)_{1-x}(BBNO)_x$ ceramics: (a) $x=0$; (b) $x=0.5$; and (c) $x=1.0$.

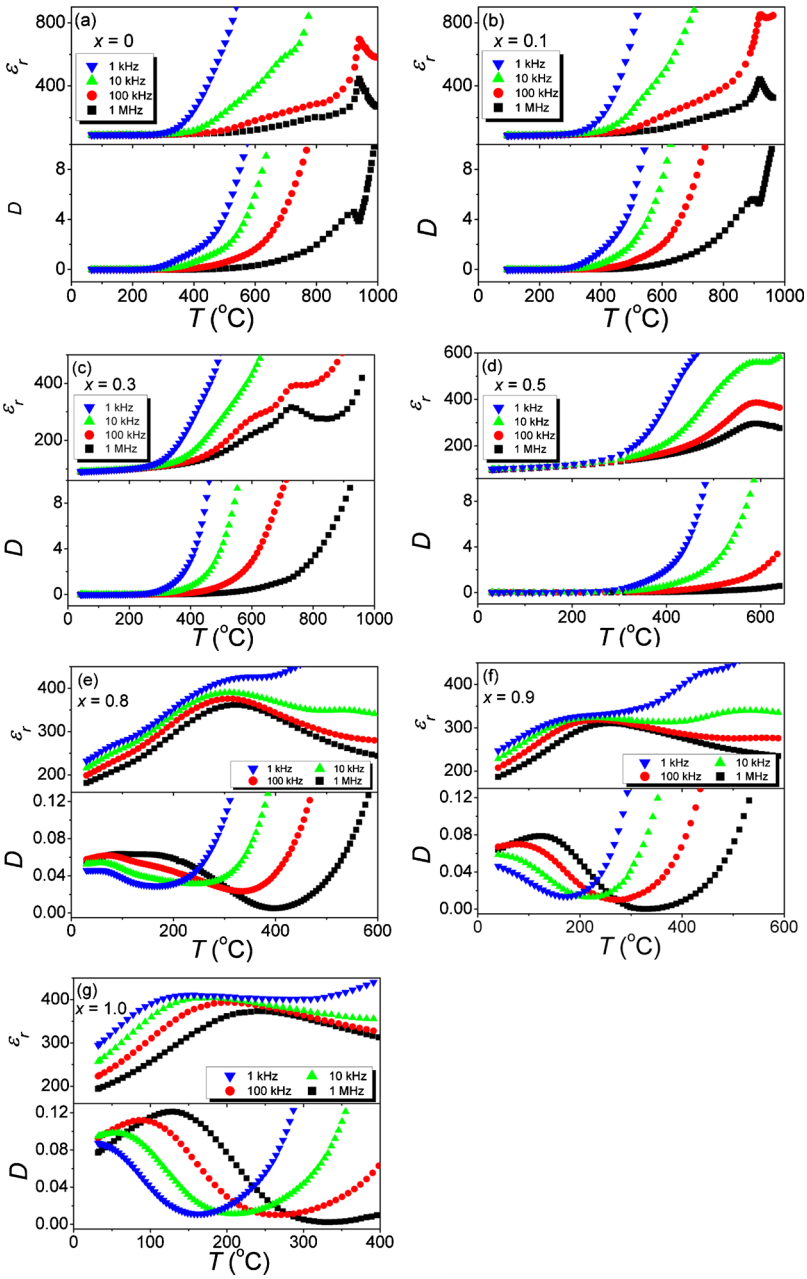

FIG. 3. (Color online) Temperature dependence of dielectric constant ε_r and loss factor D at various x values in $(CBNO)_{1-x}(BBNO)_x$ with different frequencies: (a) $x=0$; (b) $x=0.1$; (c) $x=0.3$; (d) $x=0.5$; (e) $x=0.8$; (f) $x=0.9$; and (g) $x=1.0$.

h in a nylon pot and then calcined in air at 950 °C for 4 h. The calcined powders were remilled for 24 h and admixed with about 3.0 wt % poly(ethylene glycol) as a binder. Subsequently, the powder were dried, sieved to under 500 μm, and uniaxially pressed into disks with 10 mm diameter in a steel die at a pressure of about 200 MPa. The pressed samples were sintered at 1100–1150 °C for 1 h in air. Their density was measured by the Archimedes immersion method.

TABLE II. The fitting results of relaxor compositions for V–F law [Eq. (1)] for the $(CBNO)_{1-x}(BBNO)_x$ ceramics.

x	0.8	0.9	1.0
E_a (eV)	0.11	0.11	0.56
ω_0 (Hz)	1.54×10^{11}	5.78×10^{11}	4.71×10^{13}
T_f (°C)	252	145	−173
R^2	0.9836	0.9862	0.9968

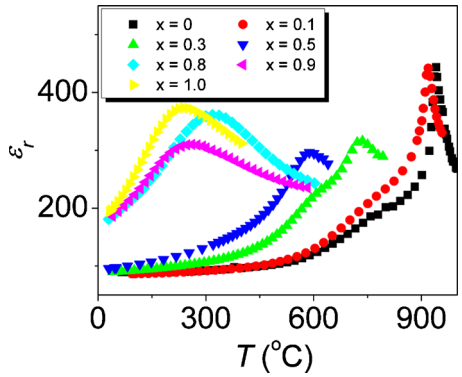

FIG. 4. (Color online) Temperature dependence of dielectric constant of $(CBNO)_{1-x}(BBNO)_x$ ceramics at the frequency of 1 MHz.

TABLE III. Characteristic ferroelectric parameters of the $(CBNO)_{1-x}(BBNO)_x$ ceramics at 1 MHz.

x	0	0.1	0.3	0.5	0.8	0.9	1.0
C_1 (K)	3.47×10^4	4.84×10^4	1.44×10^5	1.34×10^5	⋯	⋯	⋯
C_2 (K)	⋯	⋯	⋯	⋯	9.33×10^6	1.54×10^7	1.21×10^7
T_c (°C)	940	918	730	591	⋯	⋯	⋯
T_m (°C)	⋯	⋯	⋯	⋯	322	260	241
θ (°C)	845	824	284	149	⋯	⋯	⋯
γ	⋯	⋯	⋯	⋯	1.73	1.82	1.94

For each composition, there existed a temperature at which the densest ceramics were obtained. Ceramics sintered at these temperatures were chosen for final microstructure and property characterizations. Electrodes for electrical property measurements were fabricated with platinum paste (Gwent Electronic Materials Ltd, C2011004D5). The Pt electrodes were fired at 900 °C for 30 min.

X-ray diffraction (XRD) using Cu K_α radiation was performed at room temperature for crushed ceramics with a Siemens D5000 to determine the formation of the desired Aurivillius phase. The microstructures of the ceramic specimens were analyzed with a scanning electron microscope (SEM; JEOL JSM 6300). The samples for the SEM study were polished and then thermally etched at about 70 °C below their sintering temperatures for 20 min.

The temperature dependence of the dielectric constants and losses were measured at different frequencies using an LCR meter connected with high-temperature furnace (Agilent 4284A). Since the T_c or maximum dielectric constant temperature, T_m, of all of the solid solutions, $(CBNO)_{1-x}(BBNO)_x$, was higher than 200 °C, the ferroelectric $P-E$ hysteresis loops were measured at 25 and 200 °C and 10 Hz using a ferroelectric hysteresis measurement tester (NPL, U.K.).[26] The measurement procedure involved the application of triangular voltage waveforms with two complete cycles to the test samples. Samples for piezoelectric measurements were poled in silicone oil at different temperatures (100 and 200 °C) under dc electric field strengths from 8 to 11 kV/mm for 5–15 min depending on their bulk conductivities. The piezoelectric constant, d_{33}, was measured using a piezo-d_{33} meter (ZJ-3B, Institute of Acoustics, Chinese Academic of Science, Beijing).

III. RESULTS AND DISCUSSION

Table I summarizes the optimal sintering temperatures and the densities of the $(CBNO)_{1-x}(BBNO)_x$ ceramics that were used for final microstructure and property characterizations.

A. Crystal structure and morphology

XRD patterns of crushed sintered samples of $(CBNO)_{1-x}(BBNO)_x$ are presented in Figs. 1(a) and 1(b). The diffraction patterns were indexed according to the diffraction data of pure CBNO (Joint Committee on Powder Diffraction Standards No. 49-608). It can be seen from Fig. 1(a) that all the patterns are similar and the peaks at (115), (020), and (200) are shifted toward lower 2θ values with increasing BBNO content x [Fig. 1(b)]. The ceramics consisted of a single Aurivillius phase over the entire composition range without detectable secondary phases within the sensitivity of the XRD equipment. The (020) and (200) peaks of the orthorhombic structure gradually became a single peak with increasing BBNO content x, which is expected when Ca^{2+} ions are substituted by larger Ba^{2+} ions on the A-sites. The similar evolution of crystal structure has been reported in solid solution of $Bi_3TiNbO_9-BaBi_2Nb_2O_9$.[17]

Figure 2 illustrates typical SEM images of $(CBNO)_{1-x}(BBNO)_x$ ceramics. In all cases a randomly oriented platelike morphology developed. This platelike morphology is typical of Aurivillius ceramics and is due to the anisotropic nature of their crystal structure.[27]

B. Dielectric properties

The dielectric constant ε_r and loss factor D were measured as a function of temperature at different frequencies ranging from 1 kHz to 1 MHz (Fig. 3). For CBNO ($x=0$) at high frequencies (100 kHz and 1 MHz), a ferroelectric to paraelectric phase transition was apparent at 940 °C, as shown by the sharp frequency independent maximum of ε_r and the associated minimum in loss [Fig. 3(a)]. Loss peaks observed in CBNO ($x=0$) at a few degrees below the Curie point T_c [Fig. 3(a)], are ascribed to the motion of domain walls. The losses then decreased as a result of the disappearance of the ferroelectricity. Above T_c the losses increased dramatically because of increasing conductivity.[28]

The dielectric behavior for composition with $x=0.1$ [Fig. 3(b)] are similar to that of CBNO ($x=0$). There was a sharp dielectric constant peak at high frequencies ($f \geq 100$ kHz) at T_c. The samples with $x=0.3$ and 0.5 exhibited broad fre-

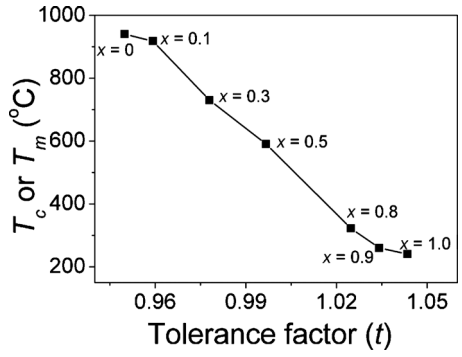

FIG. 5. Tolerance factor t vs T_c (or T_m) for $(CBNO)_{1-x}(BBNO)_x$ ceramics at 1 MHz.

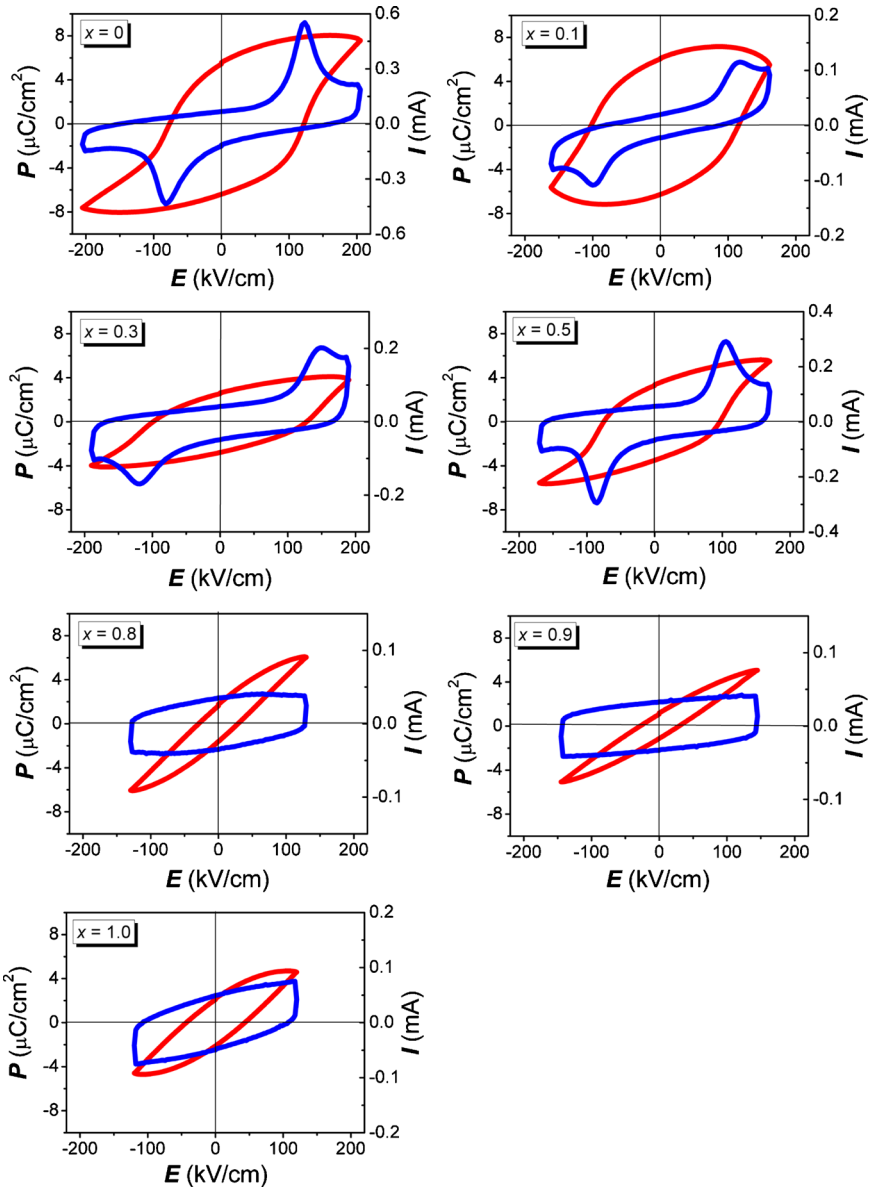

FIG. 6. (Color online) $I-E$ (blue line) and $P-E$ (red line) loops of $(CBNO)_{1-x}(BBNO)_x$ ceramics measured at 200 °C and 10 Hz.

quency independent dielectric constant peaks, as shown in Figs. 3(c) and 3(d). A similar dielectric behavior was also found for $SrBi_4Ti_4O_{15}$ doped by barium.[29]

The dielectric behavior of the compositions with $x=0.8$, 0.9, and 1.0 [Figs. 3(e)–3(g)] were very different from that of the compositions with smaller x values ($x \leq 0.5$). The following features were observed: (i) the phase transition was no longer sharp but diffuse; (ii) the temperature T_m of the maximum ε_r increased with increasing frequency and the magnitude of the ε_r decreased; and (iii) the losses exhibited a maximum at temperatures below T_m and this loss maximum was also shifted toward higher temperatures as the frequency increased. All these features are characteristic of ferroelectric relaxor behavior.[30] It is interesting to note that T_m of composition with $x=0.8$ shifts from 308 °C at 10 kHz to 322 °C at 1 MHz, which indicates it is a RFE composition with T_m temperatures higher than that of lead-based perovskite materials.

Since the frequency dispersion of relaxors does not follow the Debye law, the Vogel–Fulcher (V–F) law is used to describe the shift in the dielectric peaks with frequency[31]

$$\omega = \omega_0 \exp[-E_a/k(T-T_f)], \quad (1)$$

where ω_0 is the attempt frequency, which is associated with the cut-off frequency of the distribution of relaxation times. ω is the measurement frequency. E_a is the energy barrier for dipole switching and T_f is a freezing temperature, at which all relaxation times diverge and the distribution of relaxation times, τ, becomes infinitely long. The values of fitting parameters for relaxor compositions with $x=0.8$, 0.9, and 1.0 are shown in Table II. The fitted ω_0 values are in the frequency range of lattice vibration for ionic solids, which is of the order of $10^{11}-10^{13}$ Hz.[32] The fitted T_f temperature was 252 °C for $x=0.8$, 145 °C for $x=0.9$, and −173 °C for $x=1.0$, respectively.

Figure 4 shows the dielectric constants of $(CBNO)_{1-x}(BBNO)_x$ ceramics as a function of temperature measured at 1 MHz. It clearly shows that with increasing

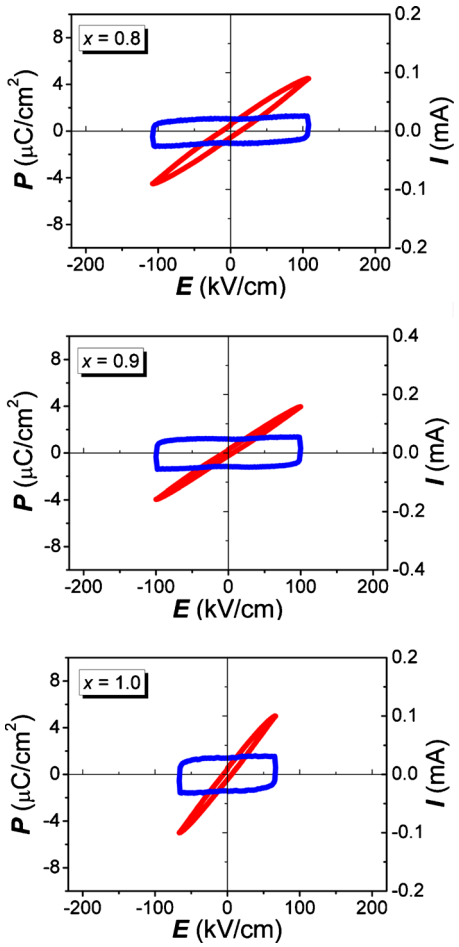

FIG. 7. (Color online) $I-E$ (blue line) and $P-E$ (red line) loops of $(CBNO)_{1-x}(BBNO)_x$ ceramics (x=0.8, 0.9, and 1.0) measured at 25 °C and 10 Hz.

barium content x on the A-sites the temperature of maximum ε_r decreased and dielectric peak became broader, which is consistent with previous studies of the effect of Ba-doping on the dielectric properties of Aurivillius materials.[21,33–36]

For compositions with x=0–0.5, the fitting parameters for the Curie–Weiss law $[\varepsilon^{-1}=(T-\theta)/C_1]$ are given in Table III. As expected for BLSFs, the Curie constants C_1 calculated from the values of the permittivity above T_c at 1 MHz are of the order of 10^4–10^5 K,[37] which suggests that $(CBNO)_{1-x}(BBNO)_x$ with x=0–0.5 are typical displacive-type ferroelectrics.[38] This is consistent with the studies on the origin of ferroelectricity in BLSFs, as mentioned early. The extrapolated Curie–Weiss temperatures θ are well below the Curie points, which can be attributed to the high losses near the Curie points. The dielectric behaviors of the compositions with $x \geq 0.8$ show a diffuse phase transition and depart from the classic Curie–Weiss law. A modified Curie–Weiss law $\varepsilon^{-1}-\varepsilon_m^{-1}=(T-T_m)^{\gamma}/C_2$ (T_m is the temperature of the maximum permittivity ε_m at a given frequency, γ=1 for normal ferroelectrics and γ=2 for ideal relaxor) is often used to fit the permittivity data.[39] The γ values obtained at 1 MHz are close to 2, confirming the relaxor nature of these compositions (Table III). The Curie constants C_2 for $x \geq 0.8$ are one or two orders of magnitude higher than the C_1 values for the

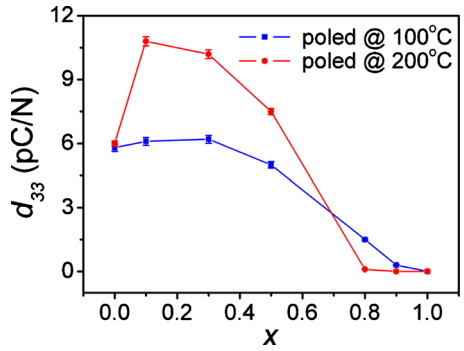

FIG. 8. (Color online) Piezoelectric coefficient (d_{33}) as a function of x for $(CBNO)_{1-x}(BBNO)_x$ ceramics poled at different temperatures (100 °C and 200 °C).

compositions with x=0–0.5, which is consistent with the previous studies on relaxor behavior in BLSFs compounds.[21,36]

It is well known that the Curie point is closely related to structural displacements.[27] The degree of distortion of the perovskite structure can be determined by the tolerance factor t, $t=(r_A+r_O)/\sqrt{2}(r_B+r_O)$, where r_A, r_B, and r_O are the ionic radii of the A and B-site cations, and an oxygen ion, respectively.[27] [r_{Ca}^{2+}=1.34 Å, r_{Ba}^{2+}=1.61 Å, CN=12; r_O^{2-}=1.40 Å, CN=6; r_{Nb}^{5+}=0.64 Å, CN=6].[22] Figure 5 shows the relationship between the tolerance factor t and T_c or T_m of the $(CBNO)_{1-x}(BBNO)_x$ system at 1 MHz. The tolerance factor t is found to increase with the increasing barium content x on the A-sites. This results in a reduction in the tilting of the NbO_6 octahedron.[27] The atomic displacements along the polar axis (a-axis) are smaller so that the energy involved to reach the prototype high-temperature structure is lowered. Accordingly, T_c or T_m decreases.

C. Ferroelectric properties

For the $(CBNO)_{1-x}(BBNO)_x$ ceramics, due to the lower limits of the attainable sample thickness (0.10–0.15 mm) produced by polishing damage, maximum current limit of the high voltage amplifier available (2.5 mA), high conductivities at high-temperature and high coercive fields (E_c), it was usually not possible to obtain saturated ferroelectric hysteresis loops. Figure 6 shows the $I-E$ and $P-E$ loops measured at 10 Hz and 200 °C for all of the compositions studied. The onset of ferroelectric domain switching, as indicated by current peaks in the $I-E$ curves, was observed for composition with $x \leq 0.5$. For compositions with $x \geq 0.8$, the currents consisted of the dielectric displacement current and conduction current with no apparant ferroelectric switching peak.[40] According to the dipolar glass model developed by Viehland *et al.*,[31] the relaxor behaviors are related to nanodomains. The remanent polarization drops quickly above T_f because thermal fluctuations destroy the correlation of the nanodomains. The fitting values of T_f for compositions with x=0.8, 0.9, and 1.0 are 252, 145, and −173 °C (Table III), respectively. The absence of domain switching in compositions with $x \geq 0.8$ is due to the fact that the test temperature (200 °C) is very close to or higher than T_f. The $I-E$ and $P-E$ loops for compositions with $x \geq 0.8$ were also measured

at 10 Hz and 25 °C, as shown in Fig. 7. However, no ferroelectric peaks were observed for any of these compositions.

D. Piezoelectric properties

Figure 8 shows the dependence of piezoelectric coefficient d_{33} for samples poled at 100 and 200 °C. When the samples were poled at 200 °C, the d_{33} value reached a maximum (10.8 pC/N) for $x=0.1$. The d_{33} value for $x=0.3$ or 0.5 was also higher than that of pure CBNO ($x=0$). The combination of high d_{33} values and high T_c points (>700 °C) suggests that the composition with $x \leq 0.3$ could be good candidates for high-temperature piezoelectric applications. The d_{33} values became zero for compositions with $x \geq 0.8$, which is consistent with absence of domain switching in the $P-E$ loops measured at 200 °C (see Fig. 6). For the samples poled at 100 °C, the d_{33} values of compositions with $x=0.8$ and 0.9 increased with respect to those poled at 200 °C. The composition with $x=0.8$ showed ferroelectricity, as evidenced by a nonzero d_{33} of 1.5 pC/N after poling at 100 °C. From the diffuse dielectric behavior [Fig. 3(e)] and the nonzero d_{33}, it has been demonstrated that the composition with $x=0.8$ is a RFE with $T_m > 300$ °C. Considering that the error of the piezo-d_{33} meter is ±0.2 pC/N, the low d_{33} value (0.3 pC/N) for the composition with $x=0.9$ suggests very weak ferroelectricity after poling at 100 °C. The existence of nonzero d_{33} for compositions with $x=0.8$ and 0.9 after poling at 100 °C is consistent with the fact that the fitted T_f values of these two compositions (see Table II) are higher than 100 °C. The d_{33} value of BBNO ($x=1.0$) was zero when poled at 100 and 200 °C, even though the samples were poled under high field of 150 kV/cm. Ando *et al.*[41] also reported that no piezoelectricity was observed in BBNO.

IV. CONCLUSION

$(CBNO)_{1-x}(BBNO)_x$ solid solution ceramics were fabricated by conventional solid-state reaction. The substitution of Ca^{2+} with the larger Ba^{2+} cation on the A-sites of the perovskite slabs produced a decrease in T_c or T_m and a broadening of the temperature maximum of the dielectric permittivity. Relaxor behavior occurred at compositions with $x \geq 0.8$. Compositions with $x \leq 0.5$ exhibited ferroelectric behavior, as evidenced by ferroelectric domain switching peaks in $I-E$ loops measured at 200 °C. The d_{33} value of CBNO ceramics can be effectively enhanced by Ba^{2+} doping on A-sites ($x \leq 0.3$). The combination of high d_{33} values and high T_c points (>700 °C) suggests that the compositions with $x \leq 0.3$ could be good candidates for high-temperature piezoelectric application. The composition with $x=0.8$ was a relaxor ferroelectric with T_m around 320 °C at 1 MHz.

[1]B. Aurivillius, Ark. Kemi **1**, 463 (1949).
[2]E. C. Subbarao, Phys. Rev. **122**, 804 (1961).
[3]C. A. P. de Araujo, J. D. Cuchiaro, L. D. McMillan, M. C. Scott, and J. F. Scott, Nature (London) **374**, 627 (1995).
[4]B. H. Park, B. S. Kang, S. D. Bu, T. W. Noh, L. Lee, and W. Jo, Nature (London) **401**, 682 (1999).
[5]D. Damjanovic, Curr. Opin. Solid State Mater. Sci. **3**, 469 (1998).
[6]A. L. Kholkin, M. Avdeev, M. E. V. Costa, J. L. Baptista, and S. N. Dorogovtsev, Appl. Phys. Lett. **79**, 662 (2001).
[7]Y. Noguchi, M. Miyayama, K. Oikawa, T. Kamiyama, M. Osada, and M. Kakihana, Jpn. J. Appl. Phys., Part 1 **41**, 7062 (2002).
[8]L. Fuentes, M. Garcia, J. Matutes-Aquino, and D. Rios-Jara, J. Alloys Compd. **369**, 10 (2004).
[9]R. E. Newnham, R. W. Wolfe, and J. F. Dorrian, Mater. Res. Bull. **6**, 1029 (1971).
[10]H. Irie, M. Miyayama, and T. Kudo, J. Appl. Phys. **90**, 4089 (2001).
[11]B. Frit and J. P. Mercurio, J. Alloys Compd. **188**, 27 (1992).
[12]K. Shibata, K. Shoji, and K. Sakata, Jpn. J. Appl. Phys., Part 1 **40**, 5719 (2001).
[13]H. Nagata, M. Itagaki, and T. Takenaka, Ferroelectrics **286**, 85 (2003).
[14]R. Aoyagi, H. Takeda, S. Okamura, and T. Shiosaki, Mater. Sci. Eng., B **116**, 156 (2005).
[15]Y. Zhu, X. Zhang, P. Gu, P. C. Joshi, and S. B. Desu, J. Phys.: Condens. Matter **9**, 10225 (1997).
[16]L. Pardo, A. Castro, P. Millán, C. Alemany, R. Jiménez, and B. Jiménez, Acta Mater. **48**, 2421 (2000).
[17]M. Nanao, M. Hirose, and T. Tsukada, Jpn. J. Appl. Phys., Part 1 **40**, 5727 (2001).
[18]S. E. Park and W. Hackenberger, Curr. Opin. Solid State Mater. Sci. **6**, 11 (2002).
[19]C. J. Stringer, N. J. Donnelly, T. R. Shrout, and C. A. Randall, J. Am. Ceram. Soc. **91**, 1781 (2008).
[20]C. J. Stringer, T. R. Shrout, and C. A. Randall, J. Appl. Phys. **101**, 054107 (2007).
[21]D. B. Jannet, M. E. Maaoui, and J. P. Mercurio, J. Electroceram. **11**, 101 (2003).
[22]R. D. Shannon, Acta Crystallogr., Sect. A: Cryst. Phys., Diffr., Theor. Gen. Crystallogr. **32**, 751 (1976).
[23]H. Yan, H. Zhang, R. Ubic, M. J. Reece, J. Liu, Z. Shen, and Z. Zhang, Adv. Mater. **17**, 1261 (2005).
[24]H. Yan, H. Zhang, R. Ubic, M. J. Reece, J. Liu, and Z. Shen, J. Mater. Sci.: Mater. Electron. **17**, 657 (2006).
[25]H. Yan, H. Zhang, M. J. Reece, and X. Dong, Appl. Phys. Lett. **87**, 082911 (2005).
[26]H. X. Yan, H. T. Zhang, Z. Zhang, R. Ubic, and M. J. Reece, J. Eur. Ceram. Soc. **26**, 2785 (2006).
[27]D. Y. Suárez, I. M. Reaney, and W. E. Lee, J. Mater. Res. **16**, 3139 (2001).
[28]K. H. Härdtl, Ceram. Int. **8**, 121 (1982).
[29]H. Oka, M. Hirose, T. Tsukada, Y. Watanabe, and T. Nomura, Jpn. J. Appl. Phys., Part 1 **39**, 5613 (2000).
[30]G. A. Samara, J. Phys.: Condens. Matter **15**, R367 (2003).
[31]D. Viehland, S. J. Jiang, L. Eric Cross, and M. Wuttig, J. Appl. Phys. **68**, 2916 (1990).
[32]W. D. Kingery, H. K. Bowen, and D. R. Uhlmann, *Introduction to Ceramics*, 2nd ed. (Wiley, New York, 1976), p. 923.
[33]G. A. Smolenskii, V. A. Isupov, and A. I. Agranovskaya, Sov. Phys. Solid State **3**, 651 (1961).
[34]N. S. Prasad and K. B. R. Varma, Mater. Res. Bull. **38**, 195 (2003).
[35]Y. Wu, M. J. Forbess, S. Seraji, S. J. Limmer, T. P. Chou, C. Nguyen, and G. Cao, J. Appl. Phys. **90**, 5296 (2001).
[36]D. B. Jennet, P. Marchet, M. E. Maaoui, and J. P. Mercurio, Mater. Lett. **59**, 376 (2005).
[37]E. C. Subbarao, J. Phys. Chem. Solids **23**, 665 (1962).
[38]E. Nakamura, T. Mitsui, and J. Euruichi, J. Phys. Soc. Jpn. **18**, 1477 (1963).
[39]S. M. Pilgrim, A. E. Sutherland, and S. R. Winzer, J. Am. Ceram. Soc. **73**, 3122 (1990).
[40]IEEE Trans. Ultrason. Ferroelectr. Freq. Control **50**, 1613 (2003).
[41]A. Ando, M. Kimura, and Y. Sakabe, Jpn. J. Appl. Phys., Part 1 **42**, 520 (2003).